STEREOELECTRONIC CONTROL IN PEPTIDE BOND FORMATION

Ab Initio Calculations and Speculations on the Mechanism of Action of Serine Proteases

DAVID G. GORENSTEIN AND KAZUNARI TAIRA
Department of Chemistry, University of Illinois at Chicago, Chicago, Illinois 60680

ABSTRACT Ab initio molecular orbital calculations have been performed on the reaction profile for the addition/elimination reaction between ammonia and formic acid, proceeding via a tetrahedral intermediate: $NH_3 + HCO_2H \rightarrow H_2NCH(OH)_2 \rightarrow NH_2CHO + H_2O$. Calculated transition state energies for the first addition step of the reaction revealed that a lone pair on the oxygen of the OH group, which is antiperiplanar to the attacking nitrogen, stabilized the transition state by 3.9 kcal/mol, thus supporting the hypothesis of stereoelectronic control for this reaction. In addition, a secondary, counterbalancing stereoelectronic effect stabilizes the second step, water elimination, transition state by 3.1 kcal/mol if the lone pair on the leaving water oxygen is not antiperiplanar to the C-N bond. The best conformation for the transition states was thus one with a lone pair antiperiplanar to the adjacent scissile bond and also one without a lone-pair orbital on the scissile bond oxygen or nitrogen antiperiplanar to the adjacent polar bond. The significance of these stereoelectronic effects for the mechanism of action of serine proteases is discussed.

INTRODUCTION

The role of orbital orientation in organic and enzymatic reactions has been of considerable current interest (Kirby, 1983; Deslongchamps, 1983; Bizzozero and Dutler, 1981; Mock, 1975; Lehn and Wipff, 1974, 1975, 1976, 1978, 1980; Radom et al., 1972; Jeffrey et al., 1972, Jeffrey and Yates, 1979; Gorenstein et al., 1977*a*, *b*, *c*, 1979, 1980). Deslongchamps and co-workers (1983) in studying tetracovalent carbon species have demonstrated selective cleavage of bonds that are *trans*-antiperiplanar (app) to lone pairs on directly bonded oxygen and nitrogen atoms. Molecular orbital calculations have provided theoretical justification for these stereoelectronic effects in tetracovalent carbon and phosphorus species and pentacovalent phosphoranes (Lehn and Wipff, 1974, 1975, 1976, 1978, 1980; Radom et al., 1972; Jeffrey et al., 1972; Jeffrey and Yates, 1979; Gorenstein et al., 1979*a*, *b*, 1979, 1980; David et al., 1973). Thus, as has been shown in molecular orbital calculations on the X_1—Y—X_2 (X = O, N; Y = P, C) structural fragments, the X_1-Y bond is strengthened (as indicated by an increase in the Mulliken overlap population), while the Y-X_2 bond is weakened when the X_1 atom lone pair is app to the Y-X_2 bond. In the *gauche*, *trans* (*g*,*t*) conformation of dimethoxymethane (Fig. 1, X = OCH_3, Y = CH_2), the overlap population for the *trans* C-O bond is 0.022 electrons lower than the overlap population for the *gauche* C-O bond. In the *g*,*t* dimethoxymethane, one lone pair (shaded in *1*) on the *gauche* bond O is app to the *trans* C-O bond, whereas no lone pairs on the *trans* bond O are app to the *gauche* bond. Thus, the weakest X_2-Y bond has one app lone pair and no lone pairs on X_2 app to the Y-X_1 bond (Gorenstein et al., 1977*b*). Lehn and Wipff (1974, 1975) and others (Radom et al., 1972; Jeffrey et al., 1972; Jeffrey and Yates, 1979) have shown similar overlap population differences in related systems.

Molecular orbital calculations on phosphate esters (Fig. 1, X_1, X_2 = OCH_3, Y = PO_2^-) have also provided confirmation for the stereoelectronic effect (Lehn and Wipff, 1974; Gorenstein et al., 1977*a*, *b*, *c*, 1979, 1980). Ab initio molecular orbital calculations (Gorenstein et al., 1979, 1980) on the reaction profile for the base-catalyzed hydrolysis of dimethylphosphate in various ester conformations have provided support for this stereoelectronic theory

$$(CH_3O)_2PO_2^- + {}^-OH \rightarrow (CH_3O)_2PO_3H^{--} \rightarrow (CH_3O)PO_3H^{--} + CH_3O^-. \quad (1)$$

Separate transition states were observed for the first addition step and the second elimination step. A metastable pentacovalent intermediate [$(CH_3O)_2PO_3H^{--}$] was established along the reaction coordinate. Significantly, for the methoxide elimination step the transition state, which has an antiperiplanar lone pair to the ethoxide leaving group, is ~11 kcal/mol lower in energy than the transition state without this app lone pair.

These calculations suggested stereoelectronic effects had a major impact on the relative energies of transition

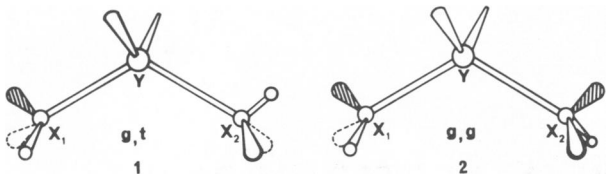

FIGURE 1 Conformations *g,t* (structure *1*) and *g,g* (structure *2*). Dihedral angles about the X_1Y and X_2Y bonds are defined by the $—X_1—Y—X_2—$ structural fragment and are *gauche* (*g*, dihedral angle ±60°) or *trans* (*t*, dihedral angle 180°). For $X_1 = X_2$ = divalent oxygen, the sp^3-hybridized lone pairs are also shown, with the antiperiplanar lone pairs (shaded).

states, much more so than on ground states or intermediates. It is thus important to use calculated transition state energies as a guide in the evaluation of the stereoelectronic effect. Although earlier calculations (Lehn and Wipff, 1974, 1975, 1976, 1978, 1980; Radom et al., 1972; Jeffrey et al., 1972; Jeffrey and Yates, 1979; Gorenstein et al., 1977*a*, *b*, *c*, 1979, 1980) supported the existence of the operation of stereoelectronic effects in tetrahedral carbon species (such as dimethoxymethane [Jeffrey and Yates, 1979; Gorenstein et al., 1977*b*]), these comparisons were based only on stable molecular structures that, again, would tend to minimize the stereoelectronic effect. Recently, a quantum mechanical study has detailed the reaction profile for the addition/elimination reaction between ammonia and formic acid, proceeding via a tetrahedral intermediate (Oie et al., 1982)

$$NH_3 + HCO_2H \rightarrow H_2NCH(OH)_2 \rightarrow NH_2CHO + H_2O. \quad (2)$$

As in the phosphate ester study, the reaction profile for reaction 2 with its well-characterized transition states is ideal for testing the stereoelectronic effect theory.

METHODS OF CALCULATION

The SCF LCAO-MO ab initio calculations used the GAUSSIAN 70 series of programs with a STO-3G minimal basis set (Hehre et al., 1969, 1974; Binkley et al., 1981). Initial structures for the addition and elimination transition states of reaction (T1 and T2), as shown in Fig. 2, were taken from the optimized structures of Oie et al. (1982). The geometry for several different conformations about the C-N and C-O-H bonds for transition states T1 and T2 (Fig. 2) were then optimized by sequentially varying all bond lengths, bond angles, and torsional angles (except C-H and O-H bond distances as shown in Table I) until the total energy had been effectively minimized when it was clear that only very small (<0.02 kcal/mol) decreases in energy were possible by further calculation. For optimization of parameter χ, the following equation (Eq. 3) was used, which assumes a parabolic harmonic vibration function

$$\chi_{OPT} = \chi_o - \frac{d\chi(E_2 - E_3)}{2(E_2 + E_3 - 2E_1)}$$

where

$$E_1 = a\chi_o^2 + b\chi_o + c$$
$$E_2 = a(\chi_o + d\chi)^2 + b(\chi_o + d\chi) + c$$
$$E_3 = a(\chi_o - d\chi)^2 + b(\chi_o - d\chi) + c. \quad (3)$$

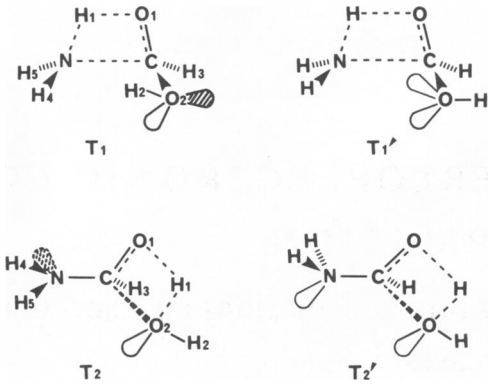

FIGURE 2 Structures for different conformations of tetrahedral transition states or intermediates in the acyl addition/elimination reaction 2 are shown. Dihedral angles about the C-N and $C-O_2$ bonds are defined by the $H_5NCO_2H_2$ structural fragment as described in Fig. 1. In T1 and T1′ the dihedral angle H_5N-CO_2 is actually closer to anticlinal (120°) although it is characterized for comparison with structure 1 (Fig. 1) as *trans*. In T2 and T2′ the dihedral angle NCO_2H_2 again is roughly anticlinal, although it is characterized as *trans*.

Since $a = (E_2 + E_3 - 2E_1)/2d\chi^2$, the force constant is negative when the numerator of coefficient *a* is negative. In those structures identified as transition states (a saddle point with only one negative force constant), the reported energy is maximized with respect to this single geometric parameter defining the reaction coordinate. All other geometric parameters are relaxed to their minimum energy value. The final geometries are given in Table I (see Figs. 2 and 3 for definition of the geometrical parameters.) Transition states have also been confirmed by the transition-state geometry optimization routine of GAUSSIAN 80 (K. Taira, unpublished results). All calculations were carried out on an IBM 4341 computer (IBM Instruments, Inc., IBM Corp., Danbury, CT).

RESULTS

Shown in Fig. 4 are the reaction profiles for formation of the amide bond in the reaction of ammonia and neutral formic acid. The profiles differ with respect to the conformations about the C-N and $C-O_2H$ bonds. The relative energies for the ground state molecules are taken from Oie et al. (1982). The relative T1 and T2 transition state energies and geometries calculated in the present study agree fairly well with the earlier calculations (Oie et al., 1982). We find T2 is 1.4 kcal/mol more stable than T1, whereas Oie et al. (1982) find T2 is 1.8 kcal/mol less stable than T1. We have not considered the concerted reaction mechanism, which Oie et al. (1982) shows was a slightly higher energy path than the stepwise process. These workers also established that the relative stabilities of the various species were generally unaffected by using more extensive basis sets and inclusion of correlation effects. Although correlation effects using second, third, or fourth Møller-Plesset perturbation theory (Binkley and Pople, 1975), and *p* polarization functions on hydrogen atoms (6-31G** basis set; Hariharan and Pople, 1973) were shown to lower the activation energies, inclusion of d-type polarization functions on heavy atoms (6-31G* basis set; Hariharan and Pople, 1975) raised the activation energies (Oie et al., 1982). The net effect of correlation and

TABLE I
STO-3G OPTIMIZED STRUCTURES OF TRANSITION STATES AND INTERMEDIATE

Parameter*	Molecule‡					
	T1	T1′	T2	T2′‖	T2a	T2a′
C—O_1	1.320 (1.315)	1.311	1.318 (1.312)	1.337	1.244	1.238
C—O_2	1.410 (1.402)	1.43	1.714 (1.720)	1.714	1.720§	1.720§
$<O_1CO_2$	118.60	119.26	87.38 (88.1)	84.481	103.88	103.63
C—N	1.751 (1.756)	1.759	1.438 (1.441)	1.466	1.474	1.475
$<NCO_1$	89.93 (89.9)	90.41	120.26 (120.6)	120.22	118.10	119.61
$<NCO_2$	107.54 (107.9)	102.67	107.25	103.69	98.49	102.48
H_1—O_1	1.467 (1.404)	1.311	—	—	—	—
H_1—O_2	—	—	1.109 (1.078)	1.109	0.990	0.997
$<H_1O_1C$	79.60 (79.8)	81.97	—	—	—	—
$<H_1O_2C$	—	—	69.04 (72.3)	68.71	116.68	114.84
τH_1O_1CN	−0.43 (−0.4)	0.53	—	—	—	—
$\tau H_1O_2CO_1$	—	—	−0.52 (−0.5)	−0.66	−60.0§	−60.0§
H_2—O_2	1.00§	1.00§	1.00§	1.0§	1.00$	1.00§
$<H_2O_2C$	104.50	103.08	114.42	111.79	112.73	117.46
τH_2O_2CN	−60.0§	180.0§	133.83	132.29	180.0§	60.0§
H_3—C	1.09§	1.09§	1.09§	1.09§	1.09§	1.09§
$<H_3CN$	105.89	106.54	114.58	113.72	115.08	112.41
$\tau H_3CO_1H_1$	−125.23	−124.90	—	—	—	—
$<H_3CO_1$	—	—	118.51	118.91	121.23	119.41
$H_{4(5)}$—N	1.01§	1.01§	1.01§	1.01§	1.01§	1.01§
$<H_4NC$	121.35	118.21	112.02	108.00	109.77	109.89
τH_4NCO_1	−110.50	114.71	—	—	—	—
τH_4NCO_2	—	—	60.0§	180.0§	60.0§	60.0§
$<H_5NC$	118.80	118.40	112.02	106.38	111.21	112.15
τH_5NCO_1	110.86	111.82	—	—	—	—
$<H_5NH_4$	—	—	109.82	104.94	109.97	107.36

*See Figs. 2 and 3 for definition of structures.
‡Bond length (X – Y or X = Y) are given ångströms, bond angles (<XYZ) and torsional angles (τWXYZ) in degrees; see Figs. 2 and 3 for atoms W, X, Y, Z. Optimized (at STO-3G level) parameters in parentheses from Oie et al., 1982.
§Assumed values.
‖Optimized parameters with C—O_2 and H_1—O_2 bond lengths fixed at same values as in the T2 transition state.

polarization was shown to lower all the activation energies equally by 4.0–5.4 kcal/mol. Most importantly, the STO-3G optimized structures gave relative energies qualitatively identical to the energies calculated from the STO-3G optimized structures but using the highest level calculations. Because we are only interested in relative energies of transition states differing only in conformation (not atomic bonding), any errors resulting from neglect of correlation and polarization in our study should essentially cancel. Optimized geometries, population analyses, and energies for various conformations of transition states T1 and T2 are shown in Tables I and II.

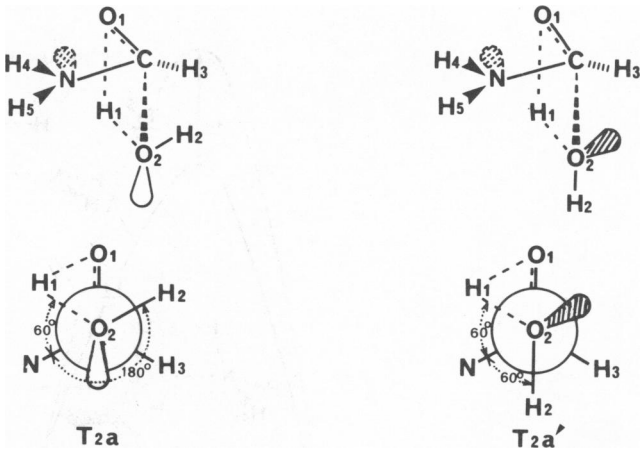

FIGURE 3 Tetrahedral structures for CO_2 bond-breaking steps differing in orientation of O_2 lone pair to the C-N bond.

DISCUSSION

Stereoelectronic Effects

The stereoelectronic effect (Kirby, 1983; Deslongchamps, 1983; Bizzozero and Dutler, 1981; Mock, 1975; Lehn and Wipff, 1974, 1975, 1976, 1978, 1980; Radom et al., 1972; Jeffrey et al., 1972; Jeffrey and Yates, 1979; Gorenstein et al., 1977*a*, *b*, *c*, 1979, 1980; David et al., 1973) is believed to arise from the interaction of an app oxygen lone pair with the σ^* antibonding X-O orbital.

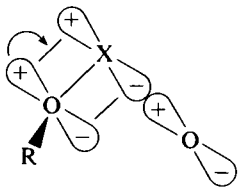

Scheme I

In terms of a simple resonance picture for the stereoelectronic effect (Kirby, 1983; Deslongchamps, 1983; Bizzozero and Dutler, 1981; Mock, 1975; Lehn and Wipff, 1974, 1975, 1976, 1978, 1980; Radom et al., 1972; Jeffrey et al., 1972; Jeffrey and Yates, 1979; Gorenstein et al., 1977*a*, *b*, *c*, 1979, 1980; David et al., 1973; Romers et al., 1969) stabilization of the structure is thought to derive from an anomeric type, double bond-no bond resonance contribution.

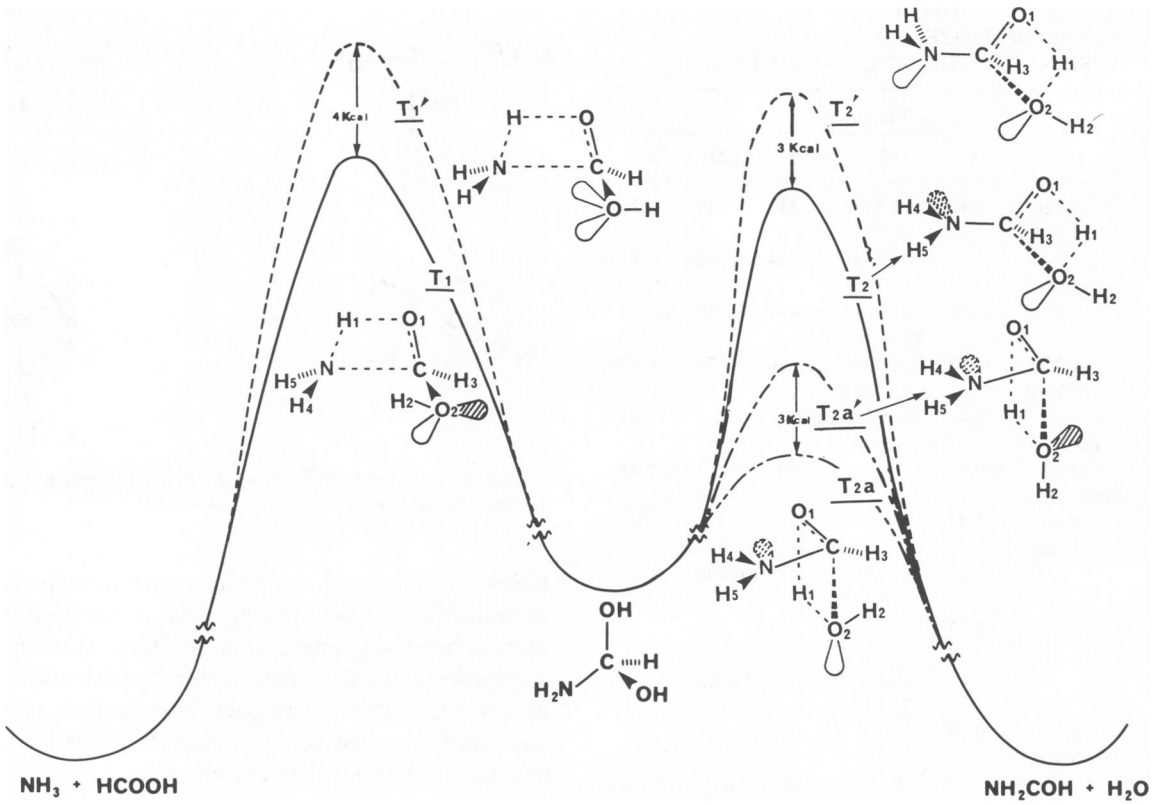

FIGURE 4 Reaction profiles for acyl addition/elimination reaction (2) are shown assuming various conformations about the C-N and C-O_2 bonds. Note only T1, T1′, and T2 optimized as transition states.

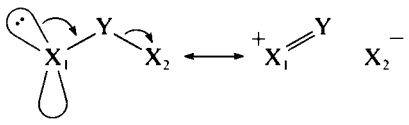

I II

Scheme II

The bond opposite to the app lone pair has some no-bond resonance character and the bond containing an app lone pair has some double-bond character.

The overlap population analysis (Mulliken, 1962) (Table II) confirms this general picture. As expected, the overlap population of a bond that is app to a lone pair is smaller than the overlap population of a bond that is not app to a lone pair (assuming we are comparing otherwise identical structures). Thus the C-N overlap population is 0.3256 in the T1′ conformation, whereas it is only 0.2066 in the T1 conformation (Table II). Note in (T1′), the unoptimized structure with identical geometry as T1 except $\tau H_2O_2CN = 180°$ as in T1′, the C-N overlap population (0.2320) is still larger than the C-N overlap population of T1. The presence of an app lone pair to the scissile C-N bond in the T1 conformation weakens this bond (reduces the overlap population). As expected from the double bond, no-bond resonance description of the stereoelectronic effect, the C—O_2 overlap population in T1 (0.5300) is larger than in T1′ (0.4974). The app lone pair on O_2 to the C-N bond in T2 imparts some double-bond character to the C-O_2 bond. Of some interest is the reduction in the H_1O_1 overlap population in the T1 conformation (0.1442) relative to the T1′ conformation. Similar overlap population stereoelectronic effects are observed for the T2 and T2′ conformations. T2, with an app lone pair on nitrogen to the scissile C-O_2 bond, has a lower C-O_2 bond overlap population (0.2232) than T2′ (0.2758, Table II).

It should be easier to break (or make, by microscopic reversibility) the bond that possesses no-bond character, and indeed as shown in Fig. 4 and Table II, this has been confirmed in these calculations. For the addition transition state (formation of the C-N bond), the conformation T1 with an oxygen lone pair on O_2H app to the C-N bond, is 3.9 kcal/mol lower in energy than T1′, which has no lone pair orbital on O_2 app to the C-N bond. Note in the following discussion we ignore the lone-pair orbitals on O_1, which will also be app to the C-N or C-O_2 bonds and hence stereoelectronically facilitate C-N or C-O_2 bond translation. As Deslongchamps (1983) has shown, selective bond cleavage in a tetrahedral intermediate requires at least two antiperiplanar lone pairs. Both T1 and T1′ were separately optimized and if the optimized geometry for T1′ were used to calculate the energy for T1, then the stereoelectronically favored transition state T1 with an app lone pair on the adjacent oxygen is 4.3 kcal/mol more stable. If the opti-

TABLE II
AB INITIO ENERGIES AND POPULATION ANALYSIS FOR VARIOUS CONFORMATIONS OF TRANSITION STATES T1 AND T2

	Conformation							
	T1	T1′	(T1′)§	T2	T2′‖	T2a	T2a′	(T2a′)§
Relative energy* (kcal/mol)	0.0‡	3.92	(7.50)	−1.39	1.48	−10.24	−7.15	(−6.35)
Bond								
C—O_1	0.6524	0.6230	0.6566	0.6270	0.5998	0.8248	0.8332	0.8332
C—O_2	0.5300	0.5974	0.5070	0.2232	0.2758	0.0664	0.0618	0.0612
C—N	0.2066	0.3256	0.2320	0.6852	0.6350	0.6370	0.6290	0.6320
H_1—O_1	0.1442	0.2704	0.1450	0.2408	0.2968	0.0038	0.0036	0.0038

*Only T1, T1′, and T2 optimized as clear transition states.
‡Total energy of T1 was −241.58587 hartrees.
§Energy and overlap populations of conformations T1′, T2′, and T2a′ with geometries identical to T1, T2, and T2a, respectively except for a single torsional angle. For (T1′) τH_2O_2CN was set at 180°, as in T1′, and for (T2a′) was set at 60°, as in T2a′.
‖ Geometry optimized T2′ except C—O_2 and H_1—O_2 bond lengths are fixed at same values as in the T2 transition state.

mized geometry for T1 were used to calculate the energy of T1′, then T1 is 7.5 kcal/mol lower in energy than T1′.

It was not possible to evaluate the stereoelectronic effect on the second transition state T2 and its conformers involving water elimination. Conformation T2 optimized properly and only one of the degrees of freedom (the C-O_2 bond length) was shown to have a negative force constant; all others were positive. We are assuming that we can approximate the 3N-6 eigenvectors and eigenvalues of the quadratic force constant matrix by treating them as classical vibrational modes (bond stretches, bends, etc.) and force constants. For a col point or transition state only one of the eigenvalues (force constants) can be negative, and this corresponds to the imaginary vibration frequency defined as the reaction coordinate. In reality, it is an oversimplification to assign a single classical vibrational mode to the reaction coordinate eigenvector. It has the advantage, however, of giving us better chemical intuition for the nature of chemical reactivity. Oie et al. (1982) and ourselves (K. Taira and D. Gorenstein, manuscript submitted for publication) have also used a more rigorous computational method for determining the transition state structures and, in support of the present method, it is significant that the reported transition state structures and energies for T1 and T2 are quite comparable with the values of Oie et al. (1982) and our own work (K. Taira and D. Gorenstein, manuscript submitted for publication). This more rigorous procedure thus serves as an important test and confirmation of the validity of our transition state search procedure. Apparently the geometric parameters are not strongly coupled and may be treated in a classical fashion. Partially geometry optimized T2′, T2a, and T2a′ were not found to be transition states (in T2a and T2a′, all force constants were positive). Note, however, in T2a and T2a′ the C-O_2 bond length was fixed at 1.72 Å and was not optimized with respect to this bond length. Although we extensively searched the reaction surface near T2′, we could not locate any structure with a single negative force constant. T2′ differs from T2 in the orientation of the nitrogen lone pair relative to the C-O_2 bond. Either we have not exhausted the energy surface to locate a transition state for conformation T2′ or indeed one does not exist. In partially optimized T2′, we first fixed bond lengths C-O_2 (1.714 Å) and H_1O_2 (1.109 Å) in T2′ to the values of transition state T2 and optimized the other geometric parameters shown in Table I. With this assumed geometry, T2′ is found to be 2.87 kcal/mol (Table II) higher energy than T2. This is again consistent with the stereoelectronic effect since T2 and not T2′ has the app lone pair on nitrogen to the scissile C-O_2 bond (T2′ has an app lone pair to C—O_2). However, this partially optimized T2′ (C-O_2 and H_{12} bond lengths not optimized) is neither a transition state nor a metastable intermediate.

Another interpretation of our failure to locate a transition state with geometry T2′ is that the stereoelectronic effect exerts such a powerful effect on these molecules that the reaction cannot proceed along a reaction pathway that does not have an app lone pair to the translating bond in the transition state. The nitrogen lone pair in T2′ is app to the nontranslating C-O_1 bond and would suggest that this is the bond which is stereoelectronically controlled to break. Recall partially optimized T2′ is not a stable structure or a transition state. If the geometry of T2′ is allowed to completely relax to its optimized structure (i.e., C-O_2 and H-O_2 bond lengths are also now optimized), bond length C-O_2 shortens and the H_1 atom transfers to O_1, regenerating the neutral intermediate. By symmetry, it is now the C-O_1 bond that must break after partial protonation of it by O_2-H. Again by symmetry, the only transition state with conformation T2′ will have a reaction coordinate (negative force constant) defined now by the C-O_1 bond length. Transition state T2 has a nitrogen app lone pair to the translating C-O_2 bond, while transition state T2′ has a nitrogen app lone pair to the translating C-O_1 bond. The orientation of the lone pair on the nitrogen determines which of the two O-H bonds breaks! This confirms Des-

longchamps' stereoelectronic effect hypothesis (Kirby, 1983; Deslongchamps, 1983).

Origin of the Stereoelectronic Effect

To further appreciate these interactions responsible for the stereoelectronic effect, we make more explicit use of one-electron molecular orbital (MO) theory, (Borden, 1975; Epiotis et al., 1977; Radom et al., 1970; Jensen and Smart, 1969; Broxton et al., 1970). The interaction of a doubly occupied MO (such as the app lone-pair orbital, ϕ_n) with a vacant MO (such as the antibonding orbital, ϕ_{σ^*}) yields a two-electron stabilization energy (Epiotis et al., 1977; Radom et al., 1970; Jensen and Smart, 1969; Broxton et al., 1970)

$$SE \sim 2K^2S^2_{n\sigma^*}/\Delta E_{n\sigma^*}. \quad (4)$$

Here, $S_{n\sigma^*}$ is the overlap integral of ϕ_n and ϕ_{σ^*} and $\Delta E_{n\sigma^*}$ is the energy separating these orbitals. From Eq. 4 this stabilization energy increases with increasing overlap, $S_{n\sigma^*}$, and decreasing energy separation, $\Delta E_{n\sigma^*}$, between the interacting orbitals. The app lone-pair stereoelectronic effect presumably derives from this orbital interaction since maximal overlap between n and σ^* is found for the app orientation (Lehn and Wipff, 1975; Radom et al., 1972; Jeffrey et al., 1972; Jeffrey and Yates, 1979; Gorenstein et al., 1977*a*, *b*, *c*, 1979, 1980; David et al., 1973; Epiotis et al., 1977; Radom et al., 1970; Jensen and Smart, 1969; Broxton et al., 1970).

We have earlier established that the stereoelectronic effect is largely a transition state phenomenon (Gorenstein et al., 1979, 1980). Thus, the energy differences between the conformations of the ground state, intermediates, or transition states of reaction 1 vary in a manner consistent with the stereoelectronic effect and Eq. 4. In dimethylphosphate the energy difference between the conformations is <1 kcal/mol. In the pentacovalent metastable dimethoxytrihydroxyphosphorane intermediate, the energy difference between the conformations is 2–6 kcal/mol. In the pentacovalent transition states the energy differences are 8–11 kcal/mol. Of course, if the stereoelectronic effect did not have its major impact in the transition state, little activation-energy differences and no kinetic acceleration would result from these interactions. From Eq. 4, increasing the distance between phosphorus and the leaving group oxygen should lower the energy of the axial σ^* orbital, hence decrease the energy separation, $\Delta E_{n\sigma^*}$, and increase the stabilization energy (SE) produced by the normal stereoelectronic effect (Gorenstein et al., 1979, 1980). In the ground state σ^* is quite high in energy, and mixing between n and σ^* via the stereoelectronic effect is minimal.

The same explanation appears to apply in the tetrahedral carbon species. Thus, at the STO-3G level, the *gauche, gauche* (*g,g*) dimethoxymethane (Fig. 1) is only 0.9 kcal/mol lower in energy than the *g,t* dimethoxymethane (Gorenstein et al., 1977*b*). The *g,g* conformation has one more app lone-pair interaction with a polar adjacent bond than the *g,t* dimethoxymethane, but it leads to <1 kcal/mol of stabilization (however, this small stereoelectronic effect is still the basis for the anomeric effect). Recall in the T1 transition state the lone pair is app to the elongated, scissile NH_3 bond (with lower σ^*) and is stabilized by 4 kcal/mol relative to the T1′ transition state.

Counterbalancing Stereoelectronic Effect

Besides weakening the bond adjacent to the app lone pair, the stereoelectronic effect will strengthen the bond containing the app lone pair (Lehn and Wipff, 1974, 1975, 1976, 1978, 1980; Gorenstein et al., 1977*a*, *b*, *c*, 1979, 1980) (what we describe as a counterbalancing stereoelectronic effect). We had earlier noted that this secondary effect is not important in pentacovalent phosphorus transition states. Thus in the transition state for methoxyl leaving in reaction 1 (Scheme I), it was found that the orientation of lone pairs on the axial methoxy group did not affect the energy of the transition state. If a lone pair on this axial oxygen were app to the basal methoxyl bond, it should be possible to the transition state through the anomeric type double bond-no bond resonance interaction of the stereoelectronic effect: the bond opposite the app lone pair has some no-bond resonance character to it.

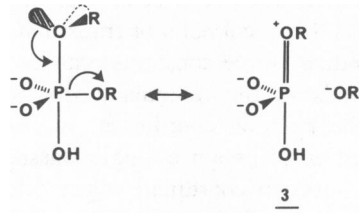

3

Scheme III

The bond containing an app lone pair has some double-bond character to it. The double-bond contribution should increase the axial bond overlap population and presumably strengthen this bond. The reason that the transition state energies in the phosphoranes are insensitive to the translating axial bond conformation likely reflects the difference in bond lengths between the basal and the scissile axial bonds. The basal methoxyl bond length is 1.67 Å, whereas the scissile apical methoxyl bond length is 2.50 Å. The orbital interaction picture for the counterbalancing stereoelectronic effect requires effective overlap of the nonbonding lone-pair orbital on the axial methoxyl oxygen with the basal methoxyl σ^* orbital (Scheme III). Increasing the separation between phosphorus and the oxygen atom bearing the lone pair will diminish this overlap, $S_{n\sigma^*}$, reduce the stabilization energy of Eq. 4, and reduce the counterbalancing stereoelectronic effect. On the other hand, increasing the distance between phosphorus and the axial oxygen

should lower the energy of the axial σ^* orbital, hence decrease the energy separation, $\Delta E_{n\sigma^*}$, and increase the *SE* produced by the normal stereoelectronic effect.[1]

The present calculations, however, do suggest that in contrast to the phosphorane transition states, the energies of the tetrahedral transition states are influenced by the counterbalancing stereoelectronic effect. As shown in Table II, T2a is 3.1 kcal/mol lower in energy than T2a'. As can be seen in Fig. 3, in T2a the O_2-H bond is app to the C-N bond, whereas in T2a' the lone pair on O_2 is app to the C-N bond. This app lone pair in T2a' produces a counterbalancing stereoelectronic effect that presumably is responsible for the higher energy of T2a'. While this *gauche* interaction would be stabilizing in the ground state, in the transition state for C-O bond breaking it is indeed destabilizing. (Another interpretation of the energy difference in T2a and T2a' is that the O_2 lone pair in T2a is app to the CO_1 bond, whereas in T2a' this lone pair is app to the C-N bond. The overlap population analysis of T2a and T2a' shows that the O_2 lone pair overlap is just about equally effective with the app C-N or C-O_1 bonds [Table II].) Presumably, the reason the counterbalancing stereoelectronic effect is important in tetrahedral carbon transition states and not in pentacovalent phosphorus transition states arises because the C-O scissile bonds are shorter than P-O scissile bonds.

In conclusion, the most stereoelectronically favored tetrahedral carbon transition state is one that possesses a lone pair app to the adjacent scissile bond while at the same time does not have a lone pair on the cleaving atom, which is app to a polar adjacent bond.

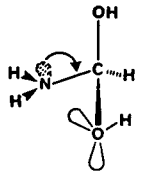

Scheme IV

This supports Lehn and Wipff's similar conclusions (1974, 1975, 1976, 1978, 1980) based upon overlap population and energy differences in tetrahedral intermediates.

Reaction Coordinate

We generally describe a reaction coordinate by the movement of the heavy atoms that undergo bond making and breaking during the reaction. Indeed for the T2 transition states, the single negative force constant describing the reaction coordinate is defined by the C-O_2 bond stretch. This is the scissile bond and agrees with our chemical intuition. Note the discussion in the Results section, however, on the caveat of assigning a classical vibrational mode to the eigenvector corresponding to the reaction coordinate.

Surprisingly, however, the single negative force constant describing the reaction coordinate for the T1 transition states is not defined by the C-N bond stretch. Although the C-N bond is the translating bond in the addition step of the reaction Eq. 2, it behaves like a normal bond with all positive force constants. The only negative force constant we find for the T1 transition state is for the H_1-O_1 bond stretch! The reaction coordinate for C-N bond making is thus represented by the position of the hydrogen atom as it transfers from the ammonia nitrogen to the carbonyl carbon. This may be quite significant (although it could also only be an artifact of the calculation or relevant only for the gas phase reaction). The importance of general acid/base catalysis in enzymatic and nonenzymatic acyl transfer reactions has long been recognized (Jencks, 1969). Our results suggest hydrogen atom movement may, indeed, be the dominant factor in certain transition states. In a full, transition-state geometry optimization (K. Taira and D. Gorenstein, manuscript submitted for publication), the reaction coordinate is defined by both C-N stretch and H atom movement.

Enzymatic Considerations

Enzymic catalysis is believed to derive from the enzyme's special capacity to stabilize (and hence lower the energy of) the transition state of the reaction (Pauling, 1946; Wolfenden, 1972; Lienhard et al., 1971). It is important to recognize, however, that for most enzymatic reactions, and certainly including peptide-bond hydrolysis, there is probably no unique transition state. Thus, as Albery and Knowles (1976) have argued, in the evolutionary perfection of an enzyme catalyst in facilitating a multistep reaction, eventually the enzyme must find a mechanism that lowers the barrier to each elementary step. Lowering the barrier to the rate-determining step will accelerate the reaction, but then any further lowering will not result in any further catalysis since another elementary step will become rate limiting. For an enzyme to achieve further catalytic efficiency it must now evolve new or better mechanisms to lower the barrier of the new rate-determining step until this step also no longer becomes rate limiting. Evolutionary pressure will thus result in an enzyme catalyzed reaction in which all of the barriers are approximately equal in height. No one step is rate limiting and, in fact, recent data support this view (Albery and Knowles, 1976).

These arguments thus suggest that an enzyme must be sufficiently conformationally flexible at its active site to

[1]On the other hand, charge-transfer effects in the transition state should partially oppose these changes. Thus, with increasing charge transfer as the scissile bond lengthens, the app lone-pair orbital on the adjacent bond O or N should lower in energy while the scissile bond σ^* orbital should raise. This will increase $E_{n\sigma^*}$ and decrease the SE. Similarly charge transfer should increase the counterbalancing stereoelectreonic effect.

stabilize each and every one of these partially rate-determining transition states. Such multiplicity of conformational states for enzymes has indeed been observed, especially in nuclear magnetic resonance (NMR) (Jardetzky and Roberts, 1981) and fast-kinetic, relaxation spectra of enzymes and enzyme complexes (Hammes and Schimmel, 1970).

Maximization of both the normal and counterbalancing stereoelectronic effects suggests that in acyl addition/elimination reactions, where both bond making in the addition step and bond breaking in the elimination step are partially rate limiting, rotation about the scissile bonds during the reaction is essential. The best stereoelectronic (and counterbalancing stereoelectronic) lone-pair orientation on N and O for C-N bond making will be the wrong orientation for optimal stereoelectronic (and counterbalancing stereoelectronic) interactions for C-O bond breaking.[2]

Thus, for C-N bond formation, stereoelectronically the lone pair on the adjacent oxygen must be app to the translating (scissile) C-N bond and no lone pair on the N should be app to the adjacent C-O bonds. This is achieved in the *t,g* conformation of transition state T1.[3] However, for C-O bond breaking, the lone pair on the adjacent nitrogen must be app to the scissile C-O bond and no lone pair on the scissile-bond oxygen should be app to the adjacent C-N bond. This is achieved in the *g,t* (see footnote 3) conformation of transition state T2. Only with rotation about the C-N and C-0_2 bonds during the reaction can the stereoelectronic effect optimally lower the activation barrier for both steps and hence lower the overall activation barrier.

This rotation during reaction is not feasible for a concerted S_N2-type displacement reaction where the rotation rate will only be a fraction of the rate of translation across the top of the energy barrier (Chesnavich and Bowers, 1976). While an app lone-pair effect could facilitate the first, largely attack phase of the reaction, the latter, largely displacement stage of a single-barrier pathway cannot be helped by the now *cis* lone pair. We expect, therefore, that the app lone-pair effect cannot play an important role in S_N2-type reactions. If, however, an intermediate, no matter how high its energy, exists along the reaction pathway, bond rotation is allowed and stereoelectronic catalysis of both bond making and breaking is possible. The intermediate need only have a lifetime of a single-bond rotation. Displacement reactions at tetrahedral carbon (S_N2 type) cannot be stereoelectronically catalyzed, whereas those at tetrahedral phosphorus (and other second- and third-row elements) may well obey these principles since pentacovalent intermediates are possible.

While app effects should not be important for carbon S_N2 reactions, they indeed operate in reactions involving trigonal or tetrahedral centers such as acyl addition/elimination reactions as shown in this paper. The tetrahedral intermediates in these reactions will generally have lifetimes long enough to permit single-bond rotation.

Several recent papers have addressed the importance of stereoelectronic effects in the mechanism of action of the serine proteases, such as α-chymotrypsin (Bizzozero and Dutler, 1981; Bizzozero and Zweifel, 1975). However, in these discussions as in all other detailed discussions of the enzymatic mechanism, no mention has been made to the important additional counterbalancing stereoelectronic effect. Chymotrypsin and most likely all other serine proteases proceed via an acyl enzyme intermediate in which formation of the acyl enzyme intermediate and hydrolysis of the intermediate in turn proceed via tetrahedral intermediates. Concentrating only on the reaction path between Michaelis complex and acyl enzyme, the enzyme must catalyze formation and breakdown of the tetrahedral intermediate in a minimum two-step reaction. If chymotrypsin is perfected, then each of these steps is partially rate limiting. Kinetic evidence supports the existence of this tetrahedral intermediate (Kraut, 1977; Fersht, 1972; Caplow, 1969). The enzyme must thus stabilize both transition states in the formation and breakdown of the tetrahedral intermediate. If stereoelectronic effects operate for one transition state, they will likely operate for both. The optimal stereoelectronic conformation for formation of the tetrahedral intermediate must, as argued above, be different from the optimal stereoelectronic conformation for breakdown of the intermediate. Passage from one transition state to the other will require single-bond rotation about C—O and C—N in the tetrahedral intermediate. We argue that a most important function of the enzyme is to provide for these conformational changes in the tetrahedral intermediate complex.

Blow (1976) has proposed a detailed stereochemical analysis for the steps in formation of the acyl enzyme that incorporates chemical modification, kinetic, and x-ray diffraction data on a number of serine proteases and their complexes. X-ray structures of stabilized pseudo-substrate intermediates (trypsin-benzamidine complex [T-B] [Huber and Bode, 1978; Bode and Schwager, 1975] and trypsin-pancreatic trypsin inhibitor complex [T-PTI] [Ruhlmann, 1973; Huber, 1974]) peptide product (AcPro-Ala-Pro-Tyr-OH) *Streptomyces griseus* protease A (Pep-SGPA) (James et al., 1980), and pseudo-tetrahedral intermediate complexes (diisopropyl phosphate-trypsin [DIP-T] [Kossiadoff and Spencer, 1981], and tosylchymotrypsin

[2]Enzymatic rate acceleration attributed to the stereoelectronic effect relative to the nonenzymatic reaction is possible because the enzyme can use binding energy to lock the substrate into the stereoelectronically optimal conformation. In solution the substrate can achieve the same conformation but only at the expense of freezing rotational degrees of freedom. Thus, any enthalpic advantage from the stereoelectronic effect will be partially canceled (in solution only) by the unfavorable entropic factor. (See Gorenstein et al., 1977*a*, *b*, *c* for additional discussion).

[3]These are approximate torsional angles for the C-N and C-0_2 bonds, respectively, with torsional angles defined in Fig. 1 (X_1 = N, X_2 = 0_2, Y = C).

[T-C] [Birktoft and Blow, 1972] and a hemiacetal complex, AcPro-Ala-Pro-Pheal-*Streptomyces griseus* protease A (James et al., 1980) are now available. In the following we wish to emphasize the additional stereochemical restrictions placed upon the mechanism resulting from the stereoelectronic requirements.

Shown in Fig. 5 is our modified description of the catalytic events in the acylation reaction as presented by Blow (1976). In summary, in *a* the trigonal amide substrate (bonds in black) binds to the substrate binding pocket to the lower right and the carbonyl oxygen near the oxyanion hole, hydrogen bonding to the backbone N-H's of serine Ser_{195} and Gly_{193}. The leaving group amide N' (grey circle) is near $N_{\epsilon 2}$ of $histidine_{57}$. Crucial to our argument as discussed by Blow and others (Blow, 1976; Brayer et al., 1979; Sielecki et al., 1979; Matthews et al., 1975, 1977) is the conformational mobility about the $C_\alpha C_\beta$ bonds of Ser_{195} and His_{57}. O_γ of Ser_{195} can be in the down (torsional angle χ_1 about C_α-C_β of Ser_{195} of $-80°$) or in the up (torsional angle χ_1 of $+90°$) (Blow, 1976; Birktoft and Blow, 1972; James et al., 1980). There exists, however, some controversy over the degree of conformational flexibility in the Ser_{195} side chain (Blow, 1976; Brayer et al., 1979; Sielecki et al., 1979; Matthews et al., 1975, 1977). Most other serine proteases appear to have the Ser_{195} side chain in the down position (χ_1 approximately equal to $-80°$). Thus, for the active site serine group, α-lytic protease has χ_1 for $-56°$ (Brayer et al., 1979), *Streptomyces griseus* serine protease has χ_1 of $-77°$ (Sielecki et al., 1979) and native subtilisin has χ_1 of $-100°$ (Matthews et al., 1977). In the latter, however, the $C_\alpha C_\beta$ bond for the active site serine (Ser_{221}) rotates by $+40°$ in going from native subtilisin to a tetrahedral intermediate boronic acid complex (Sielecki et al., 1979), which involves movement of O_γ of Ser_{221} by 1 Å. In one peptide product protease complex (Ac-Pro-Ala-Pro-Tyr-OH SGPA), Ser_{195} appears to occupy two sites. A minor occupancy site (<20%) appears to have χ_1 for Ser_{195} of $+35°$ while the major site has a normal χ_1 value of $-86°$.

The imidazole ring of His_{57} can exist in two distinct positions as well. In T-PTI complex, the imidazole ring is found in the in position (torsion angle χ_1 of $+62°$ about $C_\alpha C_\beta$ of His_{57}, whereas in T-B and T-C the imidazole ring is in the out position (χ_1 of $+92°$ and $+97°$, respectively). In the free enzyme O_γ of Ser_{195}, hydrogen bonds to $N_{\epsilon 2}$ of His_{57} (part of the much debated "charge-relay" system [Blow, 1976; Brayer et al., 1979; Sielecki et al., 1979; Matthews et al., 1975, 1977] or "proton relay" system; see Kraut, 1977) in a conformation that places it too far from the carbonyl carbon C' of the substrate. Blow provides for simple rotation about $C_\alpha C_\beta$ in a direction opposite to that depicted so as to bring C' and O_γ into bonding distances ($a \rightarrow b$, Fig. 5) in a line roughly perpendicular to the plane of the trigonal carbon C' (as required by model x-ray studies and calculations; see Burgi et al., 1973). Blow's rotation and attack would first form a tetrahedral interme-

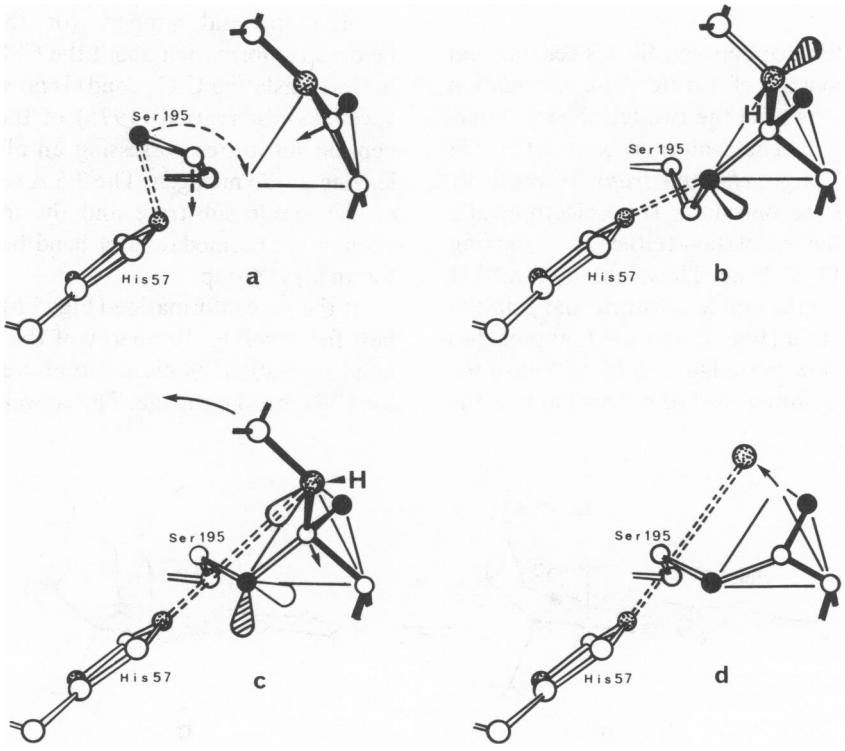

FIGURE 5 Schematic drawing of steps in acylation reaction of α-chymotrypsin partially derived from Blow (1976). Antiperiplanar lone pairs to the scissile bond are shaded.

diate closer in structure to the intermediate shown in Fig. 5 *c* except that the H-bond would still exist between O_γ Ser_{195} and His_{57} as shown in Fig. 5 *b*. Blow's conformation for *b* in Fig. 5 about C^{195}_α-C^{195}_β, C_β-O^{195}_γ, and O^{195}_γ-C′ in the HN-C_α-C_β-O_γ-C′-N′ fragment would be $-g$, $+g$, $+g$, respectively. Our opposite rotation about C_α-C^{195}_β also requires either a dip of C_β (requiring torsion about the Ser_{195} backbone) or upward, to the right movement of N′ and C′. This approach would not necessitate displacement of His_{57}, which would otherwise get too close to O_γ (as mentioned by Blow). The resulting torsional angles shown in Fig. 5 *b* about C_α-C_β, C_β-O_γ, and O_γ-C′ are $+g$, $-g$, and *t*, respectively. Without major displacements of any atoms, rotation about C_α-C_β, C_β-O_γ, and O_γ-C′ gives Fig. 5 *c* the conformation $-g$, $+g$, $+g$ (the same as Blow's intermediate, Fig. 5 *a* and *b*). The compensating opposite sense of rotation about $C_\alpha C_\beta$ and $C_\beta O_\gamma$ is similar to related pH dependent backbone movements in α-CT (Mavridis et al., 1974). Movement of His_{57} from the in position to the out position allows the hydrogen bond from $N_{\epsilon 2}$ of His_{57} to switch from the O_γ of Ser_{195} to the leaving group N′. Thus, in the in position the hydrogen bond between $N_{\epsilon 2}$ of His_{57} and O_γ of Ser_{195} is 2.7 Å and linear whereas the distance of $N_{\epsilon 2}$ to the leaving group nitrogen is too long (4.2 Å) (Bizzozero and Dutler, 1981). In the out position the hydrogen bond is between $N_{\epsilon 2}$ and the leaving group N′ (linear and 2.9 Å) (Bizzozero and Dutler, 1981). Cleavage of the scissile, C′-N′ bond and formation of the acyl-enzyme (Fig. 5 *d*) completes the first acylation steps. Addition of H_2O in *d* in Fig. 5 and reversal of the steps to *a* in Fig. 5 carries the reaction through to hydrolysis.

The only major difference between Blow's scheme and that shown in Fig. 5 consists of a different conformation about HN-C_α-C_β-O_γ-C′-N′H in the two tetrahedral intermediates *b* and *c* in Fig. 5. The conformation in *b* (Fig. 5) about C′-N and O_γ-C′ is *gauche* and *trans*, respectively (*g*,*t*), which would be the optimum, stereoelectronically favored conformation for translation (either bond making or breaking) along the O_γ-C′ bond. Thus, initially the N′-H is *trans* to the carbonyl in the amide substrate and pointing toward the $N_{\epsilon 2}$ of His_{57} in *a* (Fig. 5) and as O_γ approaches to form *b* (Fig. 5) the now pyrimidalized N′ will have the N′ lone pair (which is pointing toward solvent) app to the translating O_γ-C bond. The stereoelectronic effect will lower the energy of the transition state.

As pointed out by Bizzozero and Dutler (1981), the leaving group N′-H is pointed toward the $N_{\epsilon 2}$-H bond, which would generate dipole-dipole repulsion between these groups (another perspective for structures *b* and *c* in Fig. 5 is shown in Fig. 6). At the same time in Fig. 5 *b*, there are no lone pairs (or the incipient H-bonded lone pairs) app to the C′-N′ bond. This is required by the counterbalancing stereoelectronic effect. Our assumed conformation for the intermediate in Fig. 5 *b* differs from Bizzozero and Dutler (1981) in that it does not have a lone pair on O_γ app to the C′-N′ bond. This particular conformation eliminates the app lone-pair interaction with the C′-N′ bond (and hence eliminates any counterbalancing stereoelectronic effect). However, it is not really necessary to assume that χ_1 must have a value of $+60°$ ($+g$) in Fig. 5 *b* to minimize this counterbalancing stereoelectronic effect in the C′-O_γ bond-making transition state. A 40–60° rotation about the C′-O_γ bond (with a concomitant 40–60° counteracting rotation about Ser_{195} C_α-C_β) will also considerably reduce the app lone pair overlap with the C′-N′ bond. (Eq. 4 shows that the overlap will follow a $\cos^2\theta$ dependence of the dihedral angle, θ, between the interacting orbitals). As discussed above, χ_1 variation for Ser_{195} is just about this large in various modifications of the serine proteases. Especially notable, besides the large α-chymotrypsin χ_1 variation, is the pH dependence of trypsin's Ser_{195} χ_1, with a value of $-95°$ at pH 5 and $-60°$ at pH 8 (Huber et al., 1974).

Experimental support for the stereoelectronically favored conformation about the C′-N′ bond (app lone pair to the translating C-O_γ bond) is provided by Bizzozero and Zweifel's observation (1975) of the lack of reactivity of peptide substrates possessing an alkyl substituent on the leaving group nitrogen. The 3.5 Å separating the nitrogens of the amide substrate and the imidazole ring is large enough to accomodate a H bond but sterically impossible for an alkyl group.

If the *g*,*t* conformation (Fig. 5 *b*) is stereoelectronically best for lowering the energy of the transition state for O_γ bond formation, as discussed above, it must be the worst for C′-N′ bond cleavage. The conversion of structure *b* to *c*

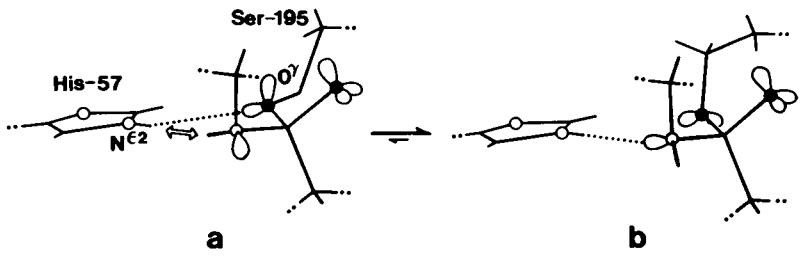

FIGURE 6 Redrawing of structures *b* and *c* of Fig. 5 to clarify app lone pairs (shaded) to C′-O_γ scissile bond (*a*) and C′-N′ scissile bond (*b*).

(Fig. 5) assumes torsion about the Ser_{195} bonds, histidine movement, and leaving-group nitrogen inversion and, in so doing, now places the $C_\beta O_\gamma$-C'-N'C fragment into the *t,g* conformation in Fig. 5 *c*. The down conformation for the Ser_{195} O_γ with $\chi_1 = -80°$ and the out position for the imidazole group are now the same as that found in the x-ray structures for the T-B and T-C complexes (Huber and Bode, 1978; Bode and Schwager, 1975; Birktoft and Blow, 1972; James et al., 1980). Movement only of the now protonated His_{57} imidazole to the out position still would not permit it to protonate the leaving group nitrogen since the N-H is pointed towards the imidazole (see Fig. 6 *a*). However, nitrogen inversion (Bizzozero and Dutler, 1981) allows the leaving group nitrogen lone pair to point towards the imidazole instead of towards the solvent. Although the O_γC'-N'-C torsional angle is still *gauche*, nitrogen N' inversion changes the O_γ-C'-N'-H torsional angles from *gauche* to *trans*. The conformation in *c* in Fig. 5 is thus described as *t,g* even through the *trans* designation refers to the O_γC'-N'-H dihedral angle. In the tetrahedral intermediates, the N'-H bond is now app to the O_γ-C' bond, whereas in *a* in Fig. 5 the lone pair was app to this bond. The stereochemistry of this N'-H bond is clearly defined by its hydrogen bonding to the carbonyl of Cys_{191}. (Blow, 1976; Brayer et al., 1979; Sielecki et al., 1979; Matthews et al., 1975, 1977). Recall in the transition state in Fig. 5 *b*, we identified the N' app lone pair to O_γ-C' as stereoelectronically controlling O_γ-C' bond translation. The *trans* N'-H to the C'-carbonyl oxygen on the planar amide system must at some stage during either the nitrogen pyrimidalization process *a* → *b* or *b* → *c* (Fig. 5) stage move from a position pointing toward His_{57} to the normal position away from His_{57} and hydrogen bonding to Cys_{191}. In the N' pyrimidal state (Fig. 5 *b* or *c*) simple nitrogen inversion suffices but in approaching the first transition state from *a* this should not be possible and the N-H should stay on the side facing His_{57} and *trans* to C'=O. The unfavorable interaction of the N' app lone pair in *b* with the carbonyl oxygen of Cys_{191} may, in fact, be yet another factor in stabilizing the first transition state. Once the intermediate *b* is formed, inversion to *c* is possible.

It must be stressed that the *g,t* → *t,g* conformational change of the tetrahedral intermediates (*b* → *c* in Fig. 5) can be achieved with minimal distortion of the enzyme or bound substrate. The proposal that the serine side group must be capable of attaining various conformations to allow for full reactivity is not unrealistic considering the known variability of its orientation in various crystalline forms as shown by x-ray diffraction studies. Thus, the χ_1 (C_α-C_β) torsional angle can vary between +93° (pH 4.5, native α-CT) (Blow, 1976; Brayer et al., 1979; Sielecki et al., 1979; Matthews et al., 1975, 1977) to −83° (in the pH 8.0, native trypsin and T-C; see Birktoft and Blow, 1972; James et al., 1980). These differ substantially from the torsional angles in the trypsin inhibitor complexes and are consistent with those proposed in *b* and *c* in Fig. 5. Thus substantial variation is possible. Together with the mechanistically required nitrogen inversion and the observed flexibility in the imidazole group, it would appear as though the serine proteases are designed to provide the stereoelectronically optimal transition states for both the acyl addition and elimination steps (Scheiner et al., 1975; Scheiner and Lipscomb, 1976; Umeyama et al., 1973).[4]

We thank the Computer Center, University of Illinois at Chicago, for generous allocation of computing time.

Support of this research by the National Science Foundation, the U.S. Army Research Office, and the National Institutes of Health is gratefully acknowledged.

Received for publication 3 February 1984.

REFERENCES

Albery, W. J., and J. R. Knowles. 1976. Evolution of enzyme function and the development of catalytic efficiency. *Biochemistry.* 15:5631–5640.

Binkley, J. S., and J. A. Pople. 1975. Møller-Plesset theory for atomic ground state energies. *Int. J. Quantum Chem. Symp.* 9:229–236

Binkley, J. S., R. A. Whiteside, R. Krishnan, R. Seeger, L. R. Kahn, and J. A. Pople. 1981. GAUSSIAN 80. Quantum Chemistry Program Exchange, Indiana University. 13:406.

Birktoft, J. J., and D. M. Blow. 1972. Structure of crystalline α chymotrypsin. V. The atomic structure of tosyl-α-chymotrypsin at 2 Å resolution. *J. Mol. Biol.* 68:187–240.

Bizzozero, S. A., and H. Dutler. 1981. Stereochemical aspects of peptide hydrolysis catalyzed by serine proteases of the chymotrypsin type. *Bioorg. Chem.* 10:46–62.

Bizzozero, S. A., and B. O. Zweifel. 1975. The importance of the conformation of the tetrahedral intermediate for the α-chymotrypsin-catalyzed hydrolysis of peptide substrates. *FEBS (Fed. Eur. Biochem. Soc.) Lett.* 59:105–108.

Blow, D. M. 1976. Structure and mechanism of chymotrypsin. *Accounts Chem. Res.* 9:145–152.

Bode, W., and P. Schwager. 1975. The refined crystal structure of bovine β-trypsin at 1.8 Å resolution. II. Crystallographic refinement, calcium binding site, benzamidine binding site and active site at pH 7.0 *J. Mol. Biol.* 98:693–717.

Borden, W. T. 1975. Modern Molecular Orbital Theory for Organic Chemists. Prentice-Hall, Englewood Cliffs, NJ. 305 pp.

Brayer, G. D., L. J. J. Delbaere, and M. N. G. James. 1979. Molecular structure of the α-lytic protease from myxobacter 495 at 2.8 Å resolution. *J. Mol. Biol.* 131:743–775.

Broxton. I. J., L. W. Deady, A. R. Katritzky, A. Lin, and R. D. Topsin. 1970. Infrared intensities as a quantitative measure of intramolecular interactions. XII. π-distortions in the ground states of some p-alkybenzenes. *J. Am. Chem. Soc.* 92:6845–6849.

Burgi, H. G., J. D. Dunitz, and E. Shefter. 1973. Geometrical reaction coordinates. II. Nucleophilic addition to a carbonyl group. *J. Am. Chem. Soc.* 95:5065–5067.

Caplow, M. 1969. Chymotrypsin catalysis. Evidence for a new intermediate. *J. Am. Chem. Soc.* 91:3639–3645.

Chesnavich, W. J., and M. I. Bowers. 1976. Statistical phase space theory of polyatomic systems. Applications to the cross section and product kinetic energy distribution of the reaction $C_2H_4\bullet^+ + C_2H_4 \rightarrow C_3H_5^+ + CH_3\bullet$. *J. Am. Chem. Soc.* 98:8301–8309.

[4]These stereoelectronic effects should now be included in a more detailed quantum mechanical calculation of the reaction profile for the serine proteases.

David, S., O. Eisenstein, W. J. Hehre, L. Salem, and R. Hoffman. 1973. Suprajacent orbital control. An interpretation of the anomeric effect. *J. Am. Chem. Soc.* 95:3806–3807.

Deslongchamps, P. 1983. Stereoelectronic Effects in Organic Chemistry. Pergamon Press, Oxford. 375 pp.

Epiotis, N. D., W. R. Cherry, S. Shaik, R. L. Yates, and F. Bernardi. 1977. Structural theory of organic chemistry. *Top. Curr. Chem.* 70:1–242.

Fersht, A. R. 1972. Mechanism of the α-chymotrypsin-catalyzed hydrolysis of specific amide substrates. *J. Am. Chem. Soc.* 94:293–295.

Gorenstein, D. G., B. A. Luxon, and J. B. Findlay. 1977*a*. Stereoelectronic effects in the reactions of phosphate diesters. Ab initio molecular orbital calculations of reaction profiles. *J. Am. Chem. Soc.* 99:8048–8049.

Gorenstein, D. G., J. B. Findlay, B. A. Luxon, and D. Kar. 1977*b*. Stereoelectronic control in carbon-oxygen and phosphorus-oxygen bond breaking processes. Ab initio calculations and speculations on the mechanism of action of ribonuclease A, staphyloccocal nuclease, and lysozyme. *J. Am. Chem. Soc.* 99:3473–3479.

Gorenstein, D. G., B. A. Luxon, J. B. Findlay, and R. Momii. 1977*c*. Stereoelectronic effects in the hydrolysis of cyclic five-membered-ring phosphate esters. Ab initio and CNDO molecular orbital calculations on alkyloxyphosphoranes. *J. Am. Chem. Soc.*. 99:4170–417.

Gorenstein, D. G., B. A. Luxon, and J. B. Findlay. 1979. Stereoeloectronic effects in the reactions of phosphate diesters. Ab initio molecular orbital calculations of reaction surfaces. 2. *J. Am. Chem. Soc.* 101:5869–5875.

Gorenstein, D. G., B. A. Luxon, and E. M. Goldfield. 1980. Stereoelectronic effects in the reactions of phosphate diesters, phosphoramidates, and phosphonates. 3. Ab initio molecular orbital calculations of transition states. *J. Am. Chem. Soc.* 102:1757–1759.

Hammes, G. G., and P. R. Schimmel. 1970. Rapid reactions and transient states. *In* The Enzymes. P. D. Boyer, editor. Academic Press, Inc., New York. Third ed. 2:67–114.

Hariharan, P. C., and J. A. Pople. 1973. The influence of polarization functions on molecular orbital hydrogenation energies. *Theor. Chim. Acta.* 28:213–222.

Hehre, W. J., R. F. Steward, and J. A. Pople. 1969. Self-consistent molecular orbital methods. I. Use of Gaussian expansions of slater-type atomic orbitals. *J. Chem. Phys.* 51:2657–2664.

Hehre, W. J., W. A. Lathan, R. Ditchfield, M. D. Newton, and J. A. Pople. 1974. GAUSSIAN 70. Quantum Chemistry Exchange Program, Indiana University. No. 236.

Huber, R., and W. Bode. 1978. Structural basis of the activation and action of trypsin. *Accounts Chem. Res.* 11:114–122.

Huber, R., D. Kukla, W. Bode, P. Schwager, K. Bartels, J. Dreisenhofer, and W. Steigemann. 1974. Structure of the complex formed by bovine trypsin and bovine pancreatic trypsin inhibitor. II. Crystallographic refinement at 1.9 Å resolution. *J. Mol. Biol.* 89:73–101.

James, M. N. G., A. R. Sielecki, G. D. Brayer, L. T. J. Delbaere, and C. -A. Bauer. 1980. Structures of product and inhibitor complexes of *Streptomyces griseus* protease A at 1.8 Å resolution. A model for serine protease catalysts. *J. Mol. Biol.* 144:43–88.

Jardetzky, O., and G. C. K. Roberts. 1981. NMR in Molecular Biology. Academic Press, Inc., New York. 681 pp.

Jeffrey, G. A., J. A. Pople, and L. Radom. 1972. The application of ab initio molecular orbital theory to the anomeric effect. A comparison of theoretical predictions and experimental data on conformations and bond lengths in some pryranoses and methyl pyranosides. *Carbohydr. Res.* 25:117–131.

Jeffrey, G. A., and J. H. Yates. 1979. Application of ab initio molecular orbital calculations to the structural moieties of carbohydrates. 4. *J. Am. Chem. Soc.* 101:820–825.

Jencks, W. P. 1969. General acid-base catalysis. *In* Catalysis in Chemistry and Enzymology. Academic Press, Inc., New York. 163–242.

Jensen, F. R., and B. E. Smart. 1969. Stabilization via carbon-carbon hyperconjugation. *J. Am. Chem. Soc.* 91:5686–5688.

Kirby, A. J. 1983. The Anomeric Effect and Related Stereoelectronic Effects at Oxygen. Springer-Verlag, Berlin. 149 pp.

Kossiakoff, A. A., and S. A. Spencer. 1981. Direct determination of the protonation states of aspartic acid-102 and histidine-57 in the tetrahedral intermediate of the serine proteases: neutron structure of trypsin. *Biochemistry.* 20:6462–6474.

Kraut, J. 1977. Serine proteases: structure and mechanism of catalysis. *Annu. Rev. Biochem.* 46:331–358.

Lehn, J. -M., and G. Wipff. 1974. Stereoelectronic properties and reactivity of the tetrahedral intermediate in amide hydrolysis. Nonempirical study of aminodihydroxymethane and relation to enzyme catalysis. *J. Am. Chem. Soc.* 96:4048–4050.

Lehn, J. -M., and G. Wipff. 1975. Stereoelectronic effects in phosphoric acid and phosphate esters. *J. Chem Soc. Chem Commun.* 800–802.

Lehn, J. -M., and G. Wipff. 1976. Stereoelectronic properties, stereospecificity, and stabilization of α-oxa and α-thia carbanions. *J. Am. Chem. Soc.* 98:7498–7505.

Lehn, J. -M., and G. Wipff. 1978. Stereoelectronic properties of tetrahdral species derived from carbonyl groups. Ab initio study of aminodihydroxymethane, $CH(OH)_2NH_2$, a model tetrahedral intermediate in amide hydrolysis. *Helv. Chim. Acta.* 61:1274–1286.

Lehn, J. -M., and G. Wipff. 1980. Stereoelectronic control in acid and base catalysis of amide hydrolysis. A theoretical study. *J. Am. Chem. Soc.* 102:1347–1354.

Lienhard, G. E., I. I. Secemsdi, K. A. Koehler, and R. N. Lindquist. 1971. Enzymatic catalysis and the transition state theory of reaction rates. Transition state analogs. *Cold Spring Harbor Symp. Quant. Biol.* 36:45–51.

Matthews, D. A., R. A. Alden, J. J. Birktoft, S. T. Freer, and J. Kraut. 1975. X-ray crystallograpic study of boronic acid adducts with subtilisin BPN (Novo). A model for the catalytic transition states. *J. Biol. Chem.* 250:7120–7126.

Matthews, D. A., R. A. Alden, J. J. Birktoft, S. T. Freer, and J. Kraut. 1977. Re-examimation of the charge relay system in subtilisin and comparison with other serine proteases. *J. Biol. Chem.* 252:8875–8883.

Mavridis, A., A. Tulinsky, and M. N. Liebman. 1974. Asymmetrical changes in the tertiary structure of α-chymotrypsin with change in pH. *Biochemistry.* 13:3661–3666.

Mock, W. L. 1975. Torsional strain considerations in the mechanism of the proteolytic enzymes, with particular application to carboxypeptidase A. *Bioorg. Chem.* 4:270–278.

Mulliken, R. S. 1962. Criteria for the construction of good self-consistent-field molecular orbital wave functions, and the significance of L.C.A.O.M.O. population analysis. *J. Chem. Phys.* 36:3428–3439.

Oie, T., G. H. Loew, S. K. Burt, J. S. Binkley, and R. D. Mac-Elroy. 1982. Quantum chemical studies of a model for peptide bond formation: formation of formamide and water from ammonia and formic acid. *J. Am. Chem. Soc.* 104:6169–6174.

Pauling, L. 1946. Molecular architecture and biological reactions. *Chem. Eng. News.* 24:1375–1377.

Radom, L., J. A. Pople, V. Buss, and P. V. R. Schleyer. 1970. Rotational barriers of alkyl cations. *J. Am. Chem. Soc.* 92:6380–6382.

Radom, L., W. J. Hehre, and J. A. Pople. 1972. Molecular orbital theory of the electronic structure of organic compounds. XIII. Fourier component analysis of internal rotation potential functions in saturated molecules. *J. Am. Chem. Soc.* 94:2371–2381.

Romers, C., C. Altona, H. R. Buys, and A. E. Havinga. 1969. Geometry and conformational properties of five- and six-membered heterocyclic compound containing oxygen or sulfur. *Top. Stereochem.* 4:39–98.

Ruhlmann, A., D. Kukla, P. Schwager, K. Bartels, and R. Huber. 1973. Structure of the complex formed by bovine trypsin and bovine pancreatic trypsin inhibitor. Crystal structure determination and stereochemistry of the contact region. *J. Mol. Biol.* 77:417–436.

Scheiner, S., D. A. Kleier, and W. N. Lipscomb. 1975. Molecular orbital studies of enzyme activity. I. Charge relay system and tetrahedral

intermediate in acylation of serine proteinases. *Proc. Natl. Acad. Sci. USA.* 72:2606–2610.

Scheiner, S., and W. N. Lipscomb. 1976. Molecular orbital studies of enzyme activity: catalytic mechanism of serine proteinases. *Proc. Natl. Acad. Sci. USA.* 73:432–436.

Sielecki, A. R., W. A. Hendrickson, C. G. Broughton, L. T. J. Delbaere, G. D. Brayer, and M. N. G. James. 1979. Protein structure refinement: *Streptomyces griseus* serine protease A at 1.8 Å resolution. *J. Mol. Biol.* 134:781–804.

Umeyama, H., A. Imamura, C. Nagata, and M. Hanano. 1973. A molecular orbital study on the enzymatic reaction mechanism of α-chymotrypsin. *J. Theor. Biol.* 41:485–502.

Wolfenden, R. 1972. Analog approaches to the structure of the transition state enzyme reactions. *Accounts Chem. Res.* 5:10–18.